

УДК 538.971

MULTIFRACTAL ANALYSIS OF AFM IMAGES OF Nb THIN FILM SURFACES¹***M.V.Altaisky, L.P.Chernenko, V.M.Balebanov², N.S.Erokhin², S.S.Moiseev²***

The multifractal analysis of the atomic Force Microscope (AFM) images of the Niobium (Nb) thin film surfaces has been performed. These Nb films are being used for the measurements of the London penetration depth of stationary magnetic field by polarized neutron reflectometry. The analysis shows the behavior of Rényi dimensions of images (in the range of available scales 6–2000 nm), like the known multifractal p -model, with typical Hausdorff dimension of prevalent color in the range of 1.6 – 1.9. This indicates the fractal nature of film landscape on those scales. The perspective of new mechanism of order parameter suppression on superconductor-vacuum boundary, manifested in anomalous magnetic field penetration, is discussed.

The investigation has been performed at the Frank Laboratory of Neutron Physics and at the Laboratory of Computing Techniques and Automation, JINR.

Мультифрактальный анализ изображений поверхности тонких ниобиевых пленок, полученных на атомном силовом микроскопе***М.В.Алтайский и др.***

Выполнен мультифрактальный анализ изображений поверхности тонких пленок Nb, полученных на атомном микроскопе. В диапазоне масштабов неоднородностей $\ell = (6 - 2000)$ нм обобщенные размерности Реньи имеют зависимость от их порядка аналогично p -модели каскадных процессов с хаусдорфовой размерностью изолиний преобладающего цвета $D_0 = 1, 6 - 1, 9$, что указывает на существенно фрактальный характер поверхности. Рассмотрено влияние фрактальности поверхности пленок на глубину проникновения магнитного поля H_0 в проводник. Для сверхпроводников глубина проникновения возрастает с увеличением фрактальной размерности. В связи с этим обсуждается возможность подавления параметра порядка на границе сверхпроводник-вакуум.

Работа выполнена в Лаборатории нейтронной физики им. И.М.Франка и Лаборатории вычислительной техники и автоматизации ОИЯИ.

¹The work was supported by RFBR under Grant 98-02-17059.

²Space Research Institute RAS, Profsoyuznaya 84/32, Moscow, 117810, Russia

1. INTRODUCTION

The thin, with thickness from 1000 nm to a few atomic layers, metallic films are being extensively used in different branches of science and technology. Their properties are being studied, both experimentally and theoretically, in relation to the superconductivity problems [1], quantum electronics, compact energy sources [2] and so on. The thin film preparation is a high technology process which requires a precise control of the deposition condition and the resulting layer parameters. The existing deposition methods, including magnetron sputtering, an electron beam evaporation, molecular beam epitaxy and others, being based on nonequilibrium processes, yield thin films with surfaces rough at nanoscales. This is *microroughness*. Since the typical microroughness scales are comparable to the scales of quantum processes occurring on the boundary of the films, the surface structure may and does affect such processes as the anomalous magnetic field penetration [1], anomalous increasing of electron emission (the Schottky effect), optical effects [3], the neutron reflectivity, etc. All these processes, as well as nonequilibrium deposition and relaxation processes, are essentially fractal [3–5], and that is why the fractal analysis of the resulting surfaces is most perspective here.

In this paper we present the results of fractal and multifractal data processing of the AFM images of Nb superconducting thin films used for polarized neutron reflectometry. The experiments have been performed at the Frank Laboratory of Neutron Physics of JINR since 1989 and devoted to the study of anomalous penetration of magnetic field \mathbf{H}_0 into the superconducting layer. The results of experiments [1] indicate the penetration depth of the magnetic field about 90 nm, which is roughly twice as great as standard theoretical estimation [6].

The typical scale of the Nb thin film surface inhomogeneity, estimated by neutron methods, is in the range of (0.5 – 10) nm, therefore the Atomic Force Microscope capable of resolving such scales was used. The visual analysis of AFM images clearly displays the heterogeneous cluster structure, see Figs. 1,2, with typical cluster size of about (20 – 70) nm for different samples. For quantitative study of the images we calculated the fractal (Hausdorff) dimension with respect to the prevalent conditional color for each image and the spectrum of Rényi dimensions also.

The remainder of the paper is organized as follows. In Sect. 2 we recall the basics of multifractal formalism. In Sect. 3 the results of the multifractal analysis of the images are presented. In Sect. 4, based on the ideas proposed in [7], we consider the possible increasing of magnetic field penetration due to the effective increasing of the metal-vacuum bound surface area for fractal ($d > 2$) surfaces. In Conclusion the possible technological applications of the results obtained and further development of the methods used are discussed.

2. MULTIFRACTAL FORMALISM

Simple box-counting method $N(\delta) \sim \delta^{-d}$ relates the dependence of the number of cells required to cover a geometrical object to their size δ . This is sufficient to describe smooth sets, such as lines and surfaces, and universal fractals (which have the same dimension anywhere), but is unfair to the objects with variable characteristics. First of all, the box-counting formalism prescribes the same weight 1 to the cells with only one point inside and

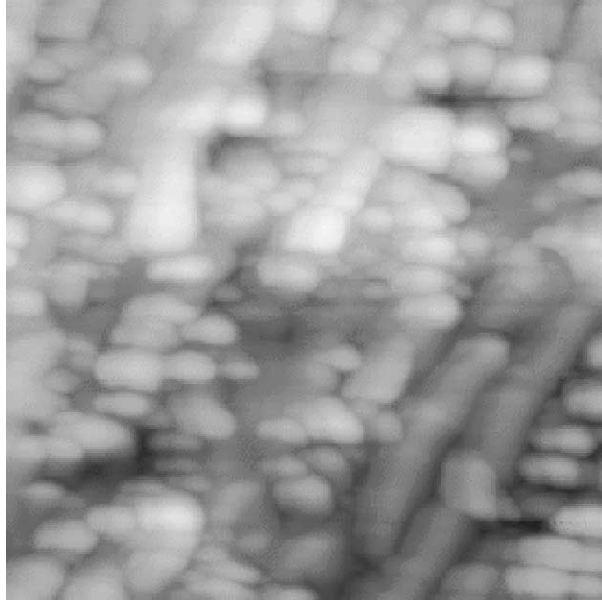


Fig. 1. The AFM image of the 700 nm (in the average) thick Nb-film. The film was prepared in Particle Physics Laboratory of JINR by electron beam evaporation. The neutron reflection roughness is 8 nm. The conditioned colors indicate the height range (0 – 40) nm (from dark-red to light-red, respectively). The AFM average roughness is 6.7 nm, which is in good agreement with neutron reflection estimation

that densely populated. To distinguish between these two polarities it was suggested [9] to use *weighted curdling* measure

$$M_d(q, \delta) = \sum_i \mu_i^q \delta^d \sim \delta^{d-\tau(q)}. \quad (1)$$

where $\mu_i = \frac{N_i}{N}$ is the ratio of the pixels of the given color within the i th cell to the total number of pixels of this color. The function $\tau(q)$, which is the scaling exponent of the q th moment of the measure μ , is often referred to as the mass exponent. For practical purposes, instead of direct calculation of the measure (1), an analog of box-counting method can be applied. First, the «partition function»

$$N(q, \delta) = \sum_i \mu_i^q \sim \delta^{-\tau(q)} \quad (2)$$

is calculated in the same way as in standard box-counting method, and then the logarithmic slope of the graph $N(q, \delta)$ versus δ gives the Rényi dimension $D_q = \tau(q)/(1 - q)$ (also introduced by Grassberger and Procaccia [8]):

$$D_q = \frac{1}{q-1} \lim_{\delta \rightarrow 0} \frac{\ln N(q, \delta)}{\ln \delta}. \quad (3)$$

The multifractal formalism was first successfully applied in physics to the description of cascade processes in hydrodynamic turbulence, for example, it is the so-called p -model [10].

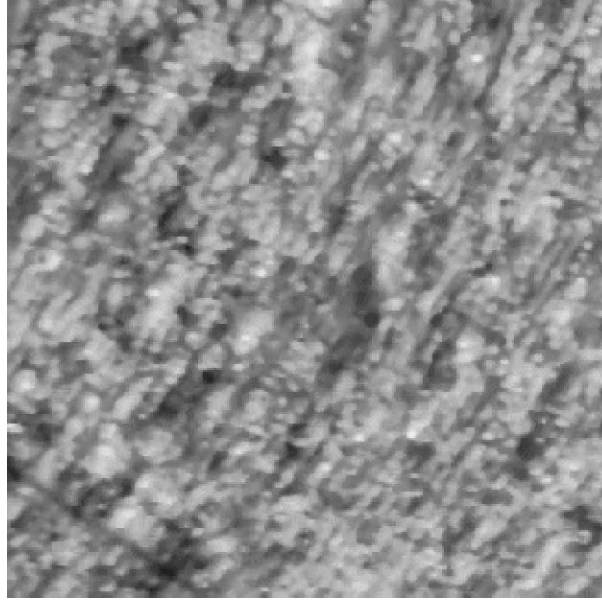


Fig. 2. The AFM image of the 265 nm (in the average) thick Nb-film. The film was prepared in Particle Physics Laboratory of JINR by electron beam evaporation. The neutron reflection roughness is 0.5 nm. The conditioned colors indicate the height range (0–37.5) nm (from dark-red to light-red, respectively). The AFM average roughness is 0.7 nm, which is in good agreement with neutron reflection estimation

Remind it briefly. The p -model describes a nonequal sharing of the energy flux from a large eddy of size l to 2^d small ones of size $l/2$, where d is space dimension. The simplest hypothesis is that a p_1 fraction of the energy goes to one half of them and a fraction $p_2 = 1 - p_1$ goes to another half. The q th moment of the energy dissipated by the eddies of a given size l can be used as a measure

$$\sum E_l^q = E_L^q \left(\frac{l}{L} \right)^{(q-1)D_q}, \quad (4)$$

where L is the maximal size of the eddies the process start with. For the n th stage of the process there will be all possible eddies

$$E_l = p_1^{n-m} p_2^m E_l, \quad m \leq n, \quad l = L/2^n,$$

and hence the Rènyi dimension can be written in the form

$$D_q = \log_2 [p_1^q + p_2^q]^{\frac{1}{1-q}}, \quad \frac{1}{2} \leq p_1 \leq 1.$$

Two limiting cases

$$D_\infty = \log_2 p_1^{-1} \quad \text{and} \quad D_{-\infty} = \log_2 p_2^{-1}$$

are of most experimental interest. They correspond to the domination of most strong and most weak domains of the cascade. The typical dependence D_q vs. q is presented in Fig.3.

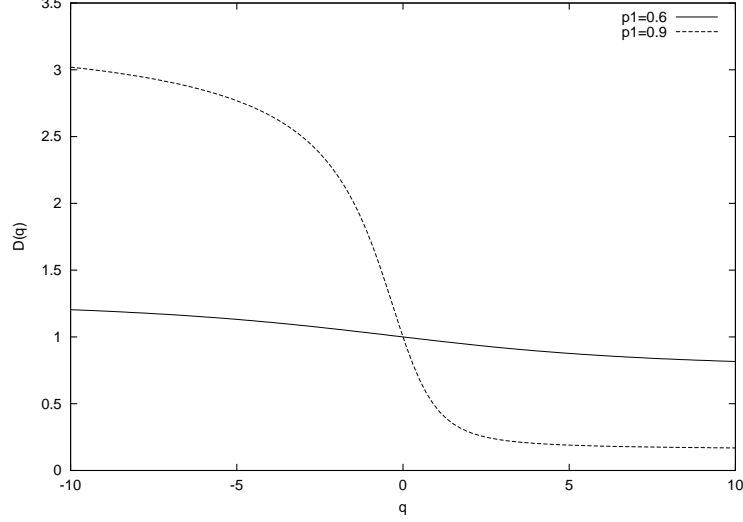


Fig. 3. The dependence of the Rényi dimensions $D(q)$ versus q in the p model for the cases: a) $p_1 = 0.6$, $p_2 = 0.4$, b) $p_1 = 0.9$, $p_2 = 0.1$

For the case of p -model $D(q)$ is decreasing function of q : $q_1 < q_2$ implies $D(q_1) > D(q_2)$. The important characteristics of the cascade processes is the singularity spectrum $f(\alpha)$, *i.e.*, the dimension of subsets I_α on the singularity strength (Lipschitz–Hölder exponent) α . To cover a fractal subset I_α (with index between α and $\alpha + d\alpha$), the number of required δ balls is given by

$$N(\alpha, \delta) = \rho(\alpha) d\alpha \delta^{-f(\alpha)}.$$

Hence, the measure (1) can be written in the form

$$M_d(q, \alpha) = \int \delta^{q\alpha - f(\alpha) + d} \rho(\alpha) d\alpha.$$

This measure is finite if the dimension d is not less than the mass exponent

$$\tau(q) = f(\alpha(q)) - q\alpha(q). \quad (5)$$

Having the mass exponents $\tau(q)$ one can express the singularity strengths $\alpha(q)$ and the dimension of their supporters by means of the Legendre transform

$$\begin{aligned} \alpha(q) &= -\frac{d}{dq} \tau(q), \\ f(\alpha) &= q\alpha + \tau(q). \end{aligned} \quad (6)$$

The maximum of $f(\alpha)$ curve corresponds to $q = 0$, *i.e.*, to the dimension of the supporter of the whole set $\cup_\alpha I_\alpha$. Thus measuring the moments of a given distribution and using the relation (6) we obtain the information about the geometry of singularities, *i.e.*, the geometry of energy dissipation if dissipative cascade processes are considered.

In general, the physics of the thin film deposition is different from that taking place in turbulence. However, for low energies, *e.g.*, for molecular epitaxy, they may be roughly described by the same Kardar–Parisi–Zhang [4] stochastic differential equation. These processes have in common the presence of self-similarity (scaling) and the existence of two limiting scales (η, L) , between which the scaling law holds. We may also suggest, that they both are universal with respect to the energy dissipation rate E (which completely determines the spectra of hydrodynamic turbulence in the Kolmogorov range (η, L)).

The problem of thin film deposition has two aspects — the dynamic and the static. The dynamic aspect is related to the quantum processes of beam interaction with the forming surface. The static problem is to describe the geometry of the formed layer using available data of observations. In our investigation we concentrate ourselves on static problem only. We consider the observed surfaces as static and study their geometry by means of multifractal analysis.

3. DATA PROCESSING RESULTS

In our data processing studies we have analyzed 8 AFM images (304x304 and 504x504 pixels format) taken with horizontal resolution from 0.4 nm/pixel to 15 nm/pixel, respectively, and height range up to 40 nm marked by about 70 conditional colors. In the table below the summary of image information is presented

Name	Size (pixels)	Resolution (nm/pixel)	Palette (colors)	Main color (R,G,B)	Count of main color	Dimension D_0
mdt0	300x303	3.1	77	(232,132,56)	6331	1.92
mdt1	302x303	0.7	68	(184,104,32)	6379	1.80
mdt2	302x302	3.8	69	(248,152,88)	6209	1.75
mdt3	302x302	15.3	75	(248,148,80)	6357	1.89
nbsi1	502x501	1.9	70	(208,116,32)	19888	1.90
nbsi2	503x504	0.4	66	(208,116,32)	18311	1.69
nbsi3	503x503	15.3	77	(224,124,48)	22687	1.91
nbsi4	502x501	2.3	69	(200,112,32)	25983	1.75

All calculations were performed for the conditional color which is dominant for each image, and thus represents the dominant height of the landscape. (We have also done some checks for other conditional colors and they show similar results). The value of D_0 (the Hausdorff box-counting dimension) is presented for all images. Below we present the geometry of prevalent colors (Figs. 4, 5) cropped from the images of Figs. 1, 2. The main color in the other images is distributed in a way similar to either of these two classes. The dependence of the Rényi dimension $D(q)$ is a typical behavior of p model. The asymptotic of $D(q)$ dimension at positive q which is about 1.5 indicates that most densely populated clusters of the given color have the isoline dimension about 1.5 and, if admit the standard hypothesis of transversal smoothness [11], the dimension of the surface is about 2.5, see Fig. 6.

4. ANOMALOUS MAGNETIC FIELD PENETRATION

The practical goal of neutron reflectometry is the precise determination of magnetic field penetration beneath the surface of the film. The results of experiments give about

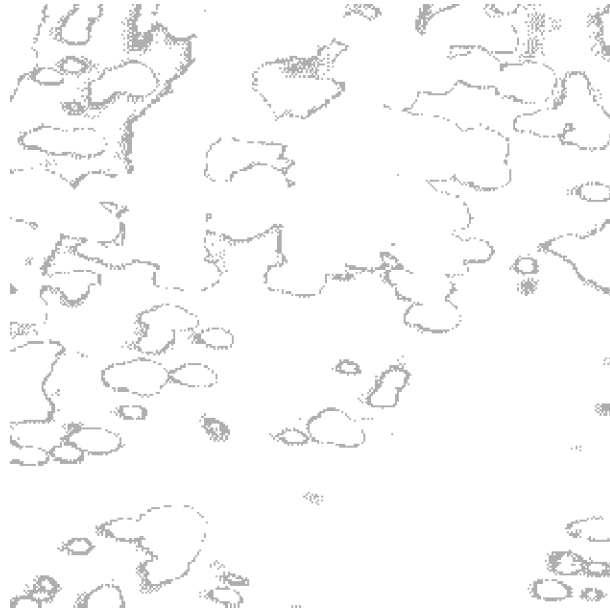


Fig. 4. The main color (248,152,88) crop of the image shown in Fig. 1

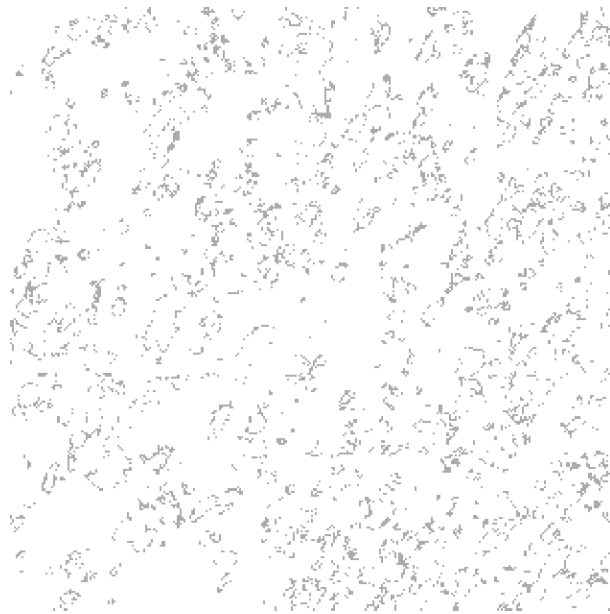


Fig. 5. The main color (248,148,80) crop of AFM image shown in Fig. 2

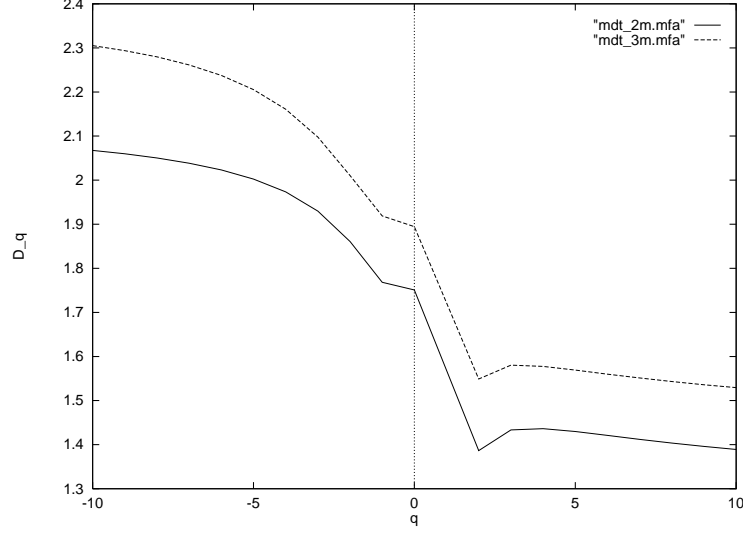


Fig. 6. D_q dimensions for high (3 nm/pix) and low (15 nm/pix) resolution samples

twice as deep penetration, that is about 90 nm [1], as expected from the London (45 nm) theory for the same experiment [6]. To study the problem let us first outline the London theory [12].

Due to the action of electric field \mathbf{E} the electrons in the metal are accelerated according to the Newton law $m_e \frac{d\mathbf{v}}{dt} = -e\mathbf{E}$, thus we have the following nonrelativistic equation for the electron current $\mathbf{j} = -en_e\mathbf{v}$:

$$\frac{d}{dt}(\Lambda\mathbf{j}) = \mathbf{E}, \quad (7)$$

where $\Lambda = \frac{m_e}{n_e e^2}$ is the London constant.

The electromagnetic fields are governed by the pair of Maxwell equations

$$\nabla \times \mathbf{E} = -\frac{1}{c} \frac{\partial \mathbf{H}}{\partial t}, \quad \nabla \times \mathbf{H} = \frac{4\pi}{c} \mathbf{j}. \quad (8)$$

Since $\nabla \cdot \mathbf{H} = 0$, applying $\nabla \times$ operation to the first of the equations (8) ($\nabla \times \nabla \times \rightarrow -\Delta$), one yields the equation for \mathbf{H}

$$\Delta \mathbf{H} - \frac{4\pi}{\Lambda c^2} \mathbf{H} = 0. \quad (9)$$

If the field $\mathbf{H} = H\mathbf{e}_y$ is parallel to the plane surface of the metal, determined by the condition $y = 0$, the equation (9) has a simple solution exponentially decaying into the metal

$$H(x) = H(0) \exp(-x/\delta), \quad (10)$$

where $\delta^2 = \frac{\Lambda c^2}{4\pi}$ is called the penetration depth.

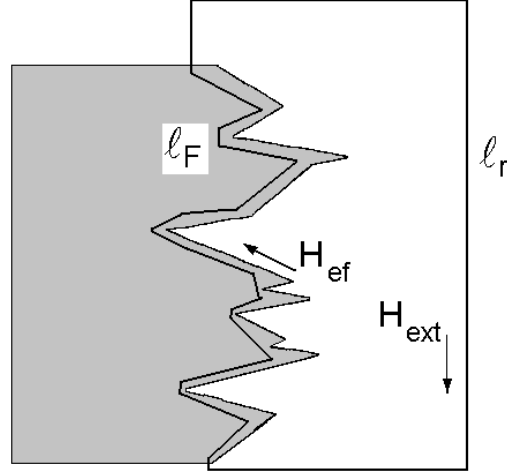


Fig. 7. The contour for the integration Eq.(11) of magnetic field circulation for fractal surface

Strictly speaking, if the (x, y) section of the surface is a nondifferentiable (fractal) curve, there is no way to apply the operation $\nabla \times \nabla \times \rightarrow -\Delta$. Instead we can only use the integral form of the second of the equations (8) like the close curve l contour integral

$$\oint \mathbf{H} d\mathbf{l} = \frac{4\pi}{c} \mathbf{I}_S, \quad (11)$$

where I_S is the current passing through the surface S with the boundary curve $\partial S = l$. Doing so, we can compare the line curve integral (11) taken along a straight line l_r (at the right in Fig. 7) with the same integral taken along the fractal curve l_F (at the left in Fig. 7). If we adopt the standard Hausdorff measure and there is no current inside $l_r + l_F$ contour, the integral should have equal values:

$$H_l \cdot L_r - \sum \delta \cdot H_{\tau k} = 0, \quad (12)$$

where L_r is the length of straight line l_r , $H_{\tau k}$ is the tangential component of magnetic field \mathbf{H} and the summation is performed over the set of boxes of size δ covering the fractal curve l_F . Averaging the equation (12) and taking into account that $\delta N(\delta) = L_F(\delta)$ is the fractal curve l_F length, we can introduce the *effective magnetic field* $H_{\text{eff}} = \langle H_{\tau k} \rangle$ acting in a metal film beneath the fractal surface:

$$H_{\text{eff}} = \frac{H_L L}{L_F(\delta) \langle \cos \phi_k \rangle}, \quad (13)$$

where ϕ_k is the angle between magnetic field direction and the tangent ort in the k th cell.

For a fractal curve its length $L_F(\delta)$ must increase when the box size δ decreases. It means that the effective magnetic field H_{eff} (13) produced by the surface current will be less in the

case of fractal curve. So, the absolute value of the total magnetic field $\mathbf{H}_t = \mathbf{H}_{\text{ext}} + \mathbf{H}_{\text{eff}}$, including the external magnetic field and that induced by surface current becomes larger. This consideration confirms the experimental result [1] on the increasing of penetration depth of the magnetic field in the case of superconducting film with fractal surface.

In fact, two concurring factors in the denominator of equation (13) are observed here: the average cosine of the tangent angle, which makes the effective field less than its «straight» counterpart, and the increasing at $\delta \rightarrow 0$ length L_δ , which decreases the effective magnetic field. Due to the complexity of presurface phenomena it is difficult to calculate which of those factors will dominate, and in general we should admit that both increasing and decreasing of the field may happen under certain condition.

It may be asked here why we use the contour integration instead of the exact form (11) with the induced surface current in the r.h.s. In fact, our consideration is not rigorous in this sense. It is demonstrative at the same extent as the derivation of the London equation (9), that is strictly valid only for harmonic fields $H, E \sim e^{i\omega t}$. What is physically true, that the density of the surface currents (induced by external magnetic field) decreases with the increasing length of the contour $i \sim L^{-1}(\delta)$. Thus, the higher is the fractal dimension of the surface, the less is local magnetic field acting *a contre* external magnetic field and contribute to H^{eff} , and the higher is the effective magnetic field H^{eff} , measured locally by neutrons. Therefore, the expected effect is the increasing of the magnetic field inside the metal with regard to the London estimation.

The consideration is valid until seriously affected by quantum effects. The rough estimation of quantum limit is the comparability of the fractal momentum $p_a = \frac{\pi\hbar}{a}$ or energy $E_a = p_a^2/(2m_e)$ with the Fermi energy. For a surface of microroughness $a = 5 \text{ nm}$ this gives $E_a \approx 0.015 \text{ eV} \ll E_{\text{Fermi}}$, while for the surface of microroughness $a = 1 \text{ nm}$ the quantum effects may be significant.

For the images presented in Fig. 1 and Fig. 2 we have reconstruct the vertical section (height) of the images using the color scale. The vertical cross sections have been performed at $x = 150$ for the images. The linear dependence of the height from the green component of the RGB color scale is assumed. The reconstructed height profiles are presented in Figs. 8, 9.

The fractal dimensions calculated for the graphs of Figs. 8, 9 are 1.36 and 1.50, respectively, but even visually the fractal nature of the landscape is clearly observed and indicates the possibility of anomalous magnetic field penetration.

Similar consideration is valid for the electric field on a fractal surface [7]. For the fractal metal surface the decreasing of the surface work function takes place. As a consequence of it, the growth of secondary electron emission stimulated by the passage of fast ions through metal films is expected. In this problem the static electric field $\mathbf{E} = -\nabla\phi$ is determined by the equation $\nabla \cdot \mathbf{E} = 4\pi\rho$, where $\rho(x, y)$ is the density of electric charge. In analogy to the consideration above, we can write

$$\oint_S \mathbf{E} \cdot d\mathbf{S} = 4\pi Q,$$

where Q is the total electric charge within the volume bounded by the surface S . Since the total charge of a metal conductor is zero the following condition holds

$$E_{n0} \cdot S_0 = \sum_k E_{nk} \cdot \Delta S_k,$$

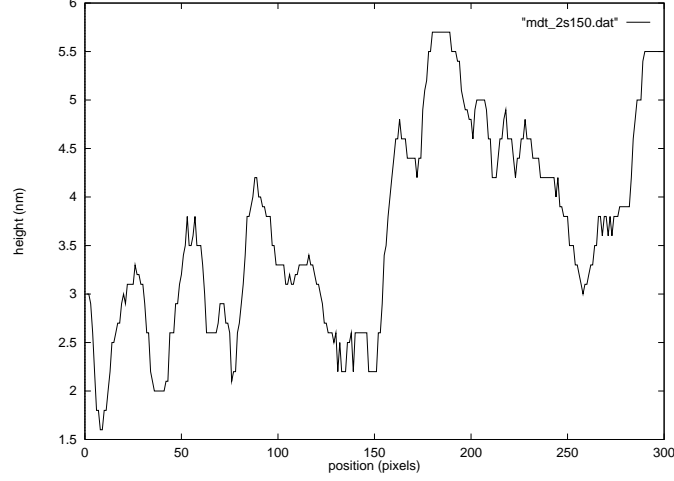


Fig. 8. The reconstructed height profile for the $x = 150$ vertical cross section of the AFM image of the Nb-film shown in Fig. 1. The film horizontal axis is in pixels, the vertical axis is in nm

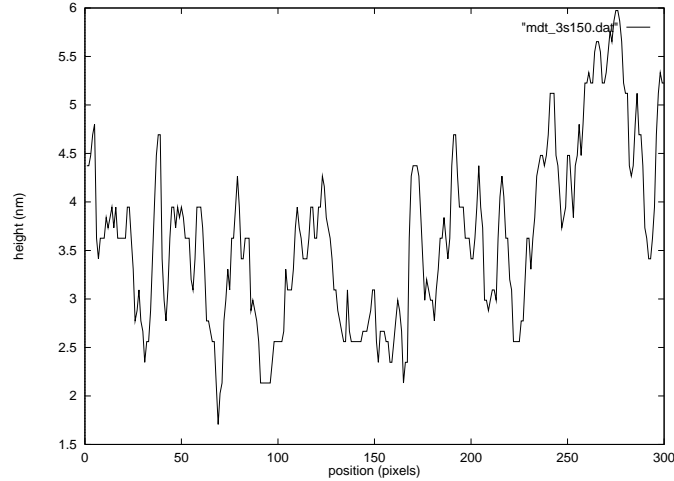


Fig. 9. The reconstructed height profile for the $x = 150$ vertical cross section of the AFM image of the Nb-film shown in Fig. 2. The film horizontal axis is in pixels, the vertical axis is in nm

where E_{nk} is the electric field component normal to the surface element ΔS_k . Therefore, for the average value of the normal component of electric field $\langle E_{nk} \rangle \equiv E_{\text{eff}}$ there is an estimation $E_{\text{eff}} = E_0 S_0 / S_F$, with S_F being the fractal surface area measured at a given scale F . Let us introduce the similarity parameter $\xi = l_{\min} / l_{\max} < 1$, and let $d_f = 2 + \beta$ ($0 < \beta < 1$) be the Hausdorff dimension of the considered fractal surface. According to [7] we have $S_0 / S_F = \xi^\beta = E_{\text{eff}} / E_0$. So, for the case of fractal conducting surface, the surface density of the electric charge decreases as $\langle \sigma_F / \sigma_0 \rangle = \xi^\beta$. The dependence of $G(\beta) = \xi^\beta$ on the parameter $\beta = d_f - 2$ in the range $0.2 < \beta < 0.8$ is given in Fig. 10 for the cases $\xi = 0.2$

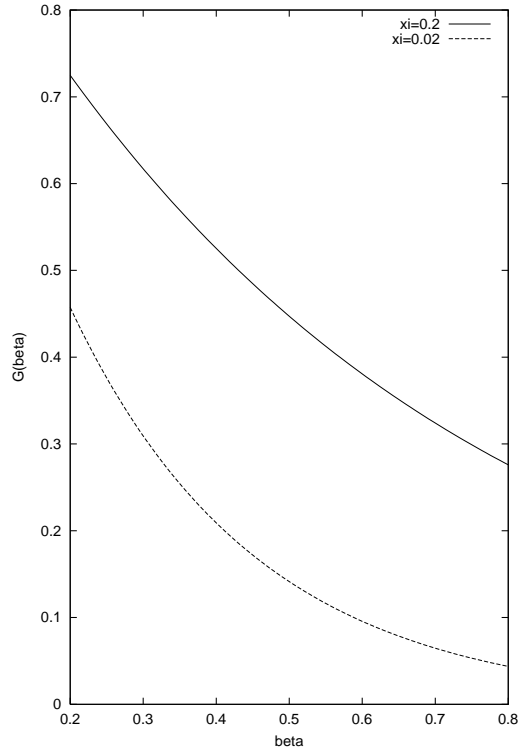


Fig. 10. The dependence of the relative magnitude of electric charge surface density $G(\beta) = \xi^\beta$ on the parameter $\beta = d_F - 2$

and $\xi = 0.02$. It is seen that higher fractal dimension d_F corresponds to the lower surface density of electric charge. This may be interpreted in terms of decreasing of surface work function.

5. CONCLUSION

In this paper the results of the analysis of Nb-films fractal properties were presented. The fractal properties of different surfaces have been already studied by means of electromagnetic wave diffraction. The idea of using neutrons for this purpose was also suggested [3]. The novelty of neutron application for fractal surface studies and of our work in general is its concentration on the problem of microstructures. The neutrons are the very instrument capable of resolving surface properties locally. Thus all technologically interesting fractal microstructures can be thoroughly investigated by neutron reflectometry. The practical application of our approach is the construction of different thin film devices where it is important to enhance, or just to control, the penetration of electric and magnetic fields beneath thin film surface. For electric field a «fractal» solution of similar type was proposed in [7]. In the present study we investigate the possible increasing of magnetic field penetration beneath metal surface. We found the experimental results on anomalous magnetic field penetration

to be in qualitative agreement with our approach based on generalization of the Stokes theorem to fractal boundaries. More rigorous quantitative study requires a detailed simulation of induced surface currents, and possibly will be done in future under certain simplifying assumptions.

We hope the methods proposed in this paper could be effectively used for thin film technologies. In particular, we plan to use these methods and software for the manufacturing of thin-film multilayer emitters for atomic batteries. For such emitters the AFM and neutron methods of control could be a technological method of controlling designed properties.

ACKNOWLEDGEMENT

The work was supported by the Russian Foundation for Basic Research, grant 98-02-17059. One of the authors (Leonid P.Chernenko) thanks Irina Dubakina and Vitali Losev, the representatives of the NT-MDT (Molecular Devices and Tools for NanoTechnology, Russia), for the AFM calibration tests of niobium samples. The authors are also thankful to Dr. D.A.Korneev for useful discussions and to Prof. V.L.Aksenov for stimulating interest to this research.

References

1. Korneev D.A. et al. — JETP Letters, 1992, v.55, p.653.
2. Balebanov V.M. et al. — Fizika Plazmi, 1998, v.24, p.789.
3. Zosimov V.V., Lamshev L.M. — Uspekhi Fiz. Nauk, 1995, v.165, p.361 (in Russian).
4. Kardar M., Parisi G., Zhang Y.C. — Phys.Rev.Lett., 1986, v.56, p.889.
5. Altaisky M.V. et al. — JINR Rapid Communications, 1997, No.2[82]-97, p.37.
6. Felcher G.P. et al. — Phys.Rev.Lett., 1984, v.52, p.1539.
7. Altaisky M.V. et al. — Preprint No.1960, Space Research Institute RAS, Moscow, 1996, p.7.
8. Grassberger P., Procaccia I. — Physica D, 1983, v.9, p.189.
9. Halsley T.C. et al. — Phys.Rev. A, 1986, v.33, p.1141.
10. Meneveau C., Sreenivasan K.R. — Phys.Rev.Lett., 1987, v.59, p.1424.
11. Feder J. — Fractals, Plenum Press, NY, 1988.
12. Landau L.D., Lifschitz E.M. — Electrodynamics of Continuous Media. Oxford, N.Y., Pergamon Press, 1960.

Received on February 15, 2000